

The magnetic structure of HoMn_2

This article has been downloaded from IOPscience. Please scroll down to see the full text article.

1992 J. Phys.: Condens. Matter 4 1559

(<http://iopscience.iop.org/0953-8984/4/6/021>)

View [the table of contents for this issue](#), or go to the [journal homepage](#) for more

Download details:

IP Address: 171.66.16.159

The article was downloaded on 12/05/2010 at 11:17

Please note that [terms and conditions apply](#).

The magnetic structure of HoMn_2

C Ritter†, R Cywinski‡, S H Kilcoyne‡ and S Mondal‡

† Institut Laue–Langevin, 38042 Grenoble Cédex, France

‡ J J Thomson Physical Laboratory, University of Reading, Reading RG6 2AF, UK

Received 10 October 1991, in final form 25 November 1991

Abstract. The crystal and magnetic structure of the C15 Laves phase of HoMn_2 was restudied using powder neutron diffraction. High-resolution spectra showed HoMn_2 to remain cubic $Fd\bar{3}m$ below the magnetic transition temperature. The Ho spins assume a spin-canted ferromagnetic structure with $7.9 \mu_B$ per Ho atom. One out of four Mn sites carries a moment of $0.6 \mu_B$ induced by the strongly polarizing magnetic environment of ferromagnetically coupled near-neighbour (111) planes of rare-earth spins. A small thermal expansion anomaly accompanied by a spin reorientation is found at the Curie point of 25 K; the Néel point of the system lies at 31 K.

1. Introduction

The magnetic moment localized at the Mn sites in the cubic C15 and hexagonal C14 $R\text{Mn}_2$ Laves-phase compounds (where R is a rare-earth metal) is inherently unstable. The magnitude of the ordered Mn moment in the antiferromagnetic state appears to be strongly correlated with the Mn–Mn near-neighbour separation, $d_{\text{Mn–Mn}}$, at distances greater than a ‘critical’ value, d_c , of approximately 2.66 Å. For $d_{\text{Mn–Mn}} < d_c$ little or no moment is observed at the Mn site, while for compounds with $d_{\text{Mn–Mn}} > d_c$, μ_{Mn} rises linearly from $2.4 \mu_B$ for TbMn_2 to $3 \mu_B$ for PrMn_2 [1]. Moreover the Néel point of these compounds is characterized by a first-order transition at which the Mn local moment collapses and the unit cell spontaneously contracts, for example by as much as 5% in the case of YMn_2 [2].

DyMn_2 has a Mn–Mn spacing which is extremely close to d_c . NMR measurements [3] had suggested the presence of two equivalent Mn sites in this C15 compound—one non-magnetic and the second possessing a moment of $2.1 \mu_B$, which is a surprising result considering that in DyMn_2 all 16 Mn sites are chemically equivalent. We have recently shown [4], using neutron powder diffraction, that this result is a consequence of the spin-canted ferromagnetic structure assumed by the Dy sublattice: 25% of the Mn sites are found to be in a strongly polarizing magnetic environment, sandwiched between ferromagnetically coupled double (111) layers of Dy spins. The Mn atoms at these sites possess a moment of $1.4 \mu_B$, while the remaining Mn atoms are at sites with magnetic inversion symmetry and carry no moment. At the ordering temperature of DyMn_2 (45 K) no first-order volume contraction is observed, providing further evidence that for this compound the Mn moments are induced rather than intrinsic.

In this paper we turn our attention to the magnetic structure of HoMn_2 , a C15 compound for which the Mn nearest-neighbour separation, $d_{\text{Mn–Mn}} = 2.64 \text{ \AA}$, is just below the critical value for the formation of an intrinsic localized Mn moment, but

for which the magnetically ordered Ho sublattice might be expected to induce a Mn moment in a fashion analogous to that found for DyMn_2 . Previous studies of HoMn_2 have provided conflicting results: NMR measurements have given zero moment [3] and $0.4 \mu_{\text{B}}$ [5] at the Mn sites, while the neutron diffraction measurements of Hardman *et al* [6] suggest a collinear ferrimagnetic structure with $8 \mu_{\text{B}}$ at the Ho sites and $-0.8 \mu_{\text{B}}$ at the Mn sites. On the other hand, in an earlier neutron study, Chamberlain [7] observed additional magnetic reflections, indexed as $h/2$, $k/2$, $l/2$, precluding such a simple ferrimagnetic model.

In order to elucidate these apparent contradictions, and in continuation of our systematic study of the nature and stability of the Mn moment in cubic RMn_2 compounds [4, 8–12], we have performed detailed high-intensity and high-resolution neutron diffraction measurements on HoMn_2 .

2. Experimental techniques

Stoichiometric HoMn_2 was prepared by melting together appropriate quantities of 99.9% pure Ho and 99.9% 'puratronic' Mn flake (both from Johnson–Matthey) in an argon-arc furnace. The resulting ingot was crushed to approximately $50 \mu\text{m}$ powder.

Neutron diffraction patterns of the powdered HoMn_2 sample were collected using the high-resolution time-of-flight diffractometer, HRPD, at the Rutherford Appleton Laboratory's ISIS neutron source, and the high intensity D1B diffractometer at the Institut Laue–Langevin, Grenoble.

HRPD has a resolution of $\Delta d/d = 8 \times 10^{-4}$, achieved by means of a long (100 m) initial flight path, thus reducing the uncertainty in the neutron time-of-flight, and by collecting the neutron diffraction spectra in backscattering geometry, for which geometrical contributions to the resolution are minimized. A time-of-flight range from 30 ms to 130 ms gave access to d spacings between 0.6 and 2.7 \AA . The HoMn_2 sample was contained in a vanadium can with planar geometry ($25 \text{ mm} \times 15 \text{ mm} \times 3 \text{ mm}$) and examined over the temperature range 4.2 K to 60 K.

D1B has a 400 element multidetector which covers an angular range of 80° in 2θ . With a monochromatic neutron wavelength of 2.52 \AA and the detector positioned at 15° , a d spacing range of $1.7 \text{ \AA} < d < 9.6 \text{ \AA}$ could be accessed with a resolution of about $\Delta d/d = 2 \times 10^{-2}$. A standard ILL 'orange' cryostat was used to vary the sample temperature in the range 1.5 K to 300 K, with typical counting times of 10 minutes per spectrum.

3. Results

3.1. Crystal structure

High-resolution spectra using HRPD above and below the magnetic transition temperature gave no indication for a structural distortion of HoMn_2 at low temperatures (figure 1). The structure remains cubic with $Fd\bar{3}m$ symmetry. This has to be compared to the low-temperature tetragonal distortion of YMn_2 , the monoclinic one found for TbMn_2 and the rhombohedral one present in DyMn_2 [12]. Structural analysis of the HRPD diffraction patterns using the CAILS programme [13] yield lattice parameters of $7.4594(2) \text{ \AA}$ and $7.4614(1) \text{ \AA}$ at 5 K and 60 K, respectively. It should be noted in figure 1 that the Bragg reflections both above and below the ordering

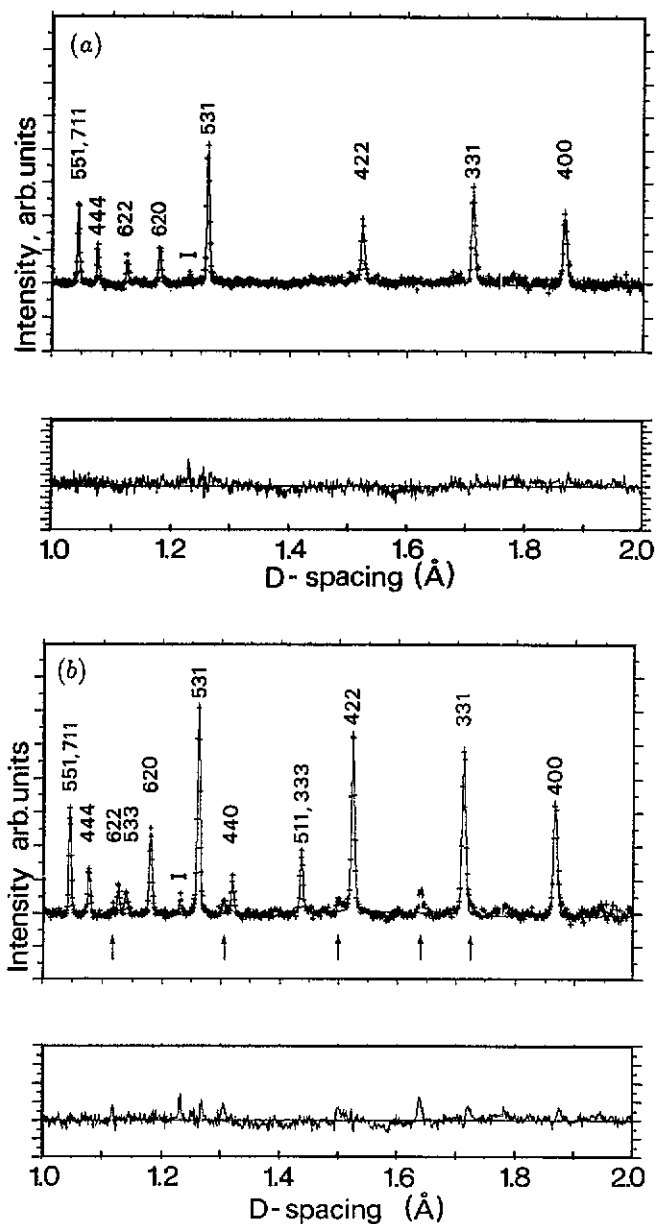


Figure 1. Sections of the HRPD diffraction patterns from HoMn_2 at (a) 40 K and (b) 5 K. The solid lines are refinements using the $Fd\bar{3}m$ space group; difference plots are shown below. Magnetic intensity appears both at the nuclear Bragg positions and in satellites (arrows) at low temperature.

temperature show significant line broadening over the linewidths expected from the resolution function. The effect is more clearly seen in figure 2 where the (331) Bragg reflection from HoMn_2 is compared with that calculated using the instrumental resolution. This broadening can be interpreted in terms of internal strain within the sample, indicating a value for the strain of $e = 2 \times 10^{-3}$. As will be discussed, this

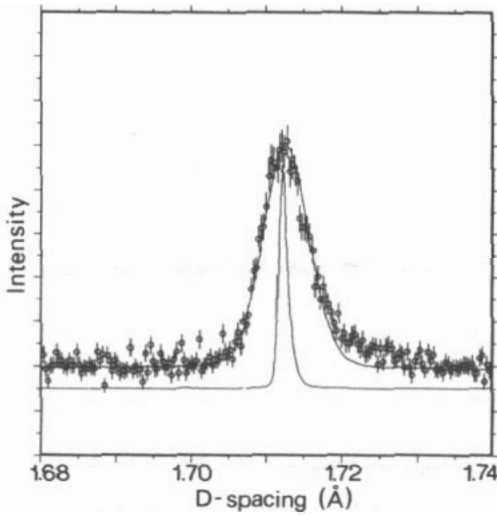


Figure 2. Fit of the nuclear (331) reflection of HoMn_2 together with the instrumental resolution.

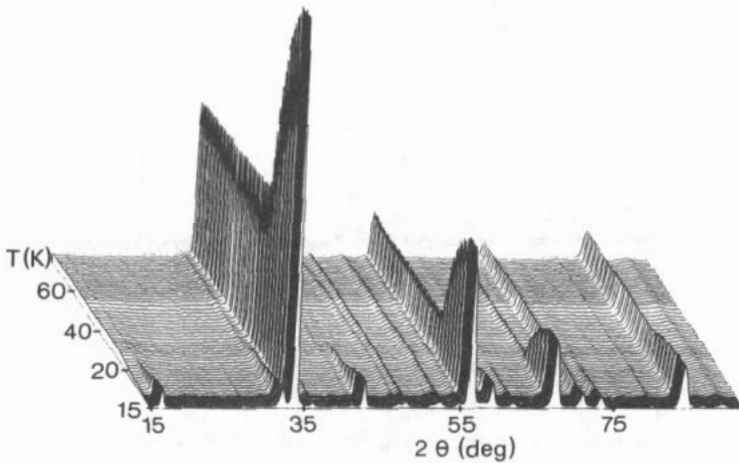


Figure 3. Evolution of the neutron diffraction pattern ($\lambda = 2.52 \text{ \AA}$) between 1.5 K and 76 K. Antiferromagnetic and ferromagnetic components can be seen at low temperature.

internal strain might play a role in defining the low-temperature magnetic structure of HoMn_2 . Large magnetic contributions to the nuclear Bragg peaks appear below the transition temperature. However, as already observed by Chamberlain [7], small additional lines show up as well at intermediate positions. This precludes the ferrimagnetic model as proposed by Hartman [6] and demanded the detailed analysis of the true magnetic ground state.

3.2. Magnetic structure

The thermal evolution of the diffraction pattern of HoMn_2 between 1.5 K and 76 K as measured on D1B is shown in the thermogram of figure 3. As the temperature

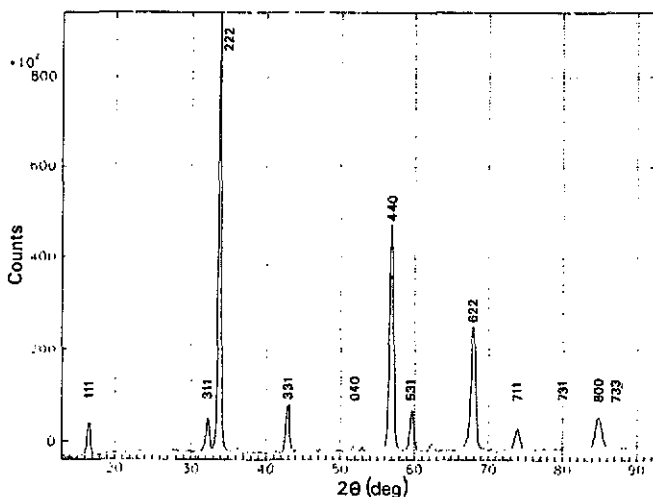


Figure 4. Difference spectrum (1.5 K–34 K) of HoMn_2 indexed using the double cubic unit cell.

decreases, the onset of long-range magnetic order is clearly visible near to 30 K: at this temperature the nuclear peaks of the original cubic unit cell begin to increase in intensity revealing a predominantly ferromagnetic component of the magnetic scattering. Additional Bragg reflections of much lower intensity (indicative of a further antiferromagnetic component) also appear. Figure 4 shows the difference between spectra collected at 1.5 K and 34 K: all peaks can be indexed on a unit cell which is double that of the original cell in all three directions. In this scheme the peaks associated with the antiferromagnetic compound all have odd indices (111,311,331...) indicating a magnetic structure not dissimilar to that reported for DyMn_2 [4]. Figure 5(a) displays the temperature variation of the integrated intensity of the (222) nuclear Bragg peak (indexed as (111) on the original unit cell). The Curie point is found to be close to 28 K. Figure 5(b) shows a similar plot for the antiferromagnetic (331) reflection. Its disappearance at 31 K is preceded by an increase in intensity at 25 K, suggestive of a spin reorientation at this temperature. Sequential refinement of the nuclear cell volume as a function of temperature (figure 6) reveals that the thermal expansion deviates slightly from linearity at 25 K. This may be related either to the spin reorientation or to the Curie temperature itself. However, no first-order discontinuity in the cell volume at T_c , such as that observed for compounds with $d_{\text{Mn}-\text{Mn}} > d_c$, is observed.

Table 1. Results of the Rietveld refinement for HoMn_2 at 1.5 K. k_x , k_y and k_z are components of μ . For a picture of the magnetic structure see reference [4].

$\mu_{\text{Ho}} (\mu_B)$	k_x	k_y	k_z	$\mu_{\text{Mn}} (\mu_B)$	k_x	k_y	k_z
7.8(1)	7.0(1) ^a	-1.9(1)(+1.9) ^b	+2.9(1)(-2.9) ^b	0.6(2)	—	0.6(2)(-0.6)	-0.1(2)(+0.1)
$a (\text{Å})$	$b (\text{Å})$	$c (\text{Å})$	R_{BRAGG}	R_p	R_{WP}	R_{NUC}	R_{MAG}
5.277(1)	10.553(2)	14.914(3)	7.6	10.3	10.4	5.4	8.8

^a \equiv Ferromagnetic component. ^b \equiv Antiferromagnetic component

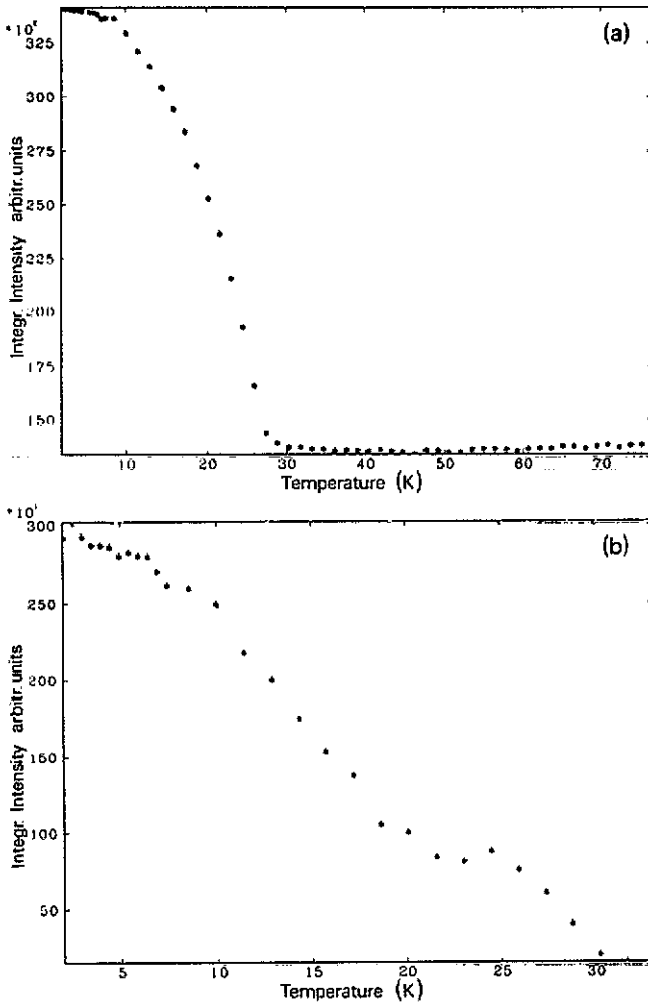


Figure 5. (a) Integrated intensity of the nuclear (222) peak between 1.5 K and 76 K. The magnetic contribution disappears at about 28 K. (b) Integrated intensity of the magnetic (331) peak between 1.5 K and 35 K. A spin reorientation sets in about 25 K; the peak disappears at about 31 K. Peaks are indexed using the double cubic unit cell.

These results clearly indicate that the behaviour of HoMn_2 is closely related to that of DyMn_2 . We might therefore expect that the spin-canted ferromagnetic order of the rare-earth sublattice may remove the degeneracy of the initially equivalent Mn sites. Assuming that the spin orientations of the Ho atoms are similar to those determined for Dy in DyMn_2 , we have used a modified Rietveld program [14] to refine the low-temperature spectra. Instead of using the large unit cell based on a doubling of the nuclear cell in all three directions, we have chosen an orthorhombic cell with $a = (1/2)a_i + (1/2)a_j$, $b = -a_i + a_j$, and $c = 2a_k$, where a_i , a_j and a_k define the original cube edges. An initial fit, which assumes only magnetic moments at the Ho site, could be substantially improved by assuming a magnetic moment on every fourth Mn site (figure 7). The attempt to refine a magnetic moment on all Mn sites orientated antiparallel to the ferromagnetic component of the Ho moment—the ferrimagnetic model proposed by Hardman *et al* [6]—proved unsuccessful. Table 1

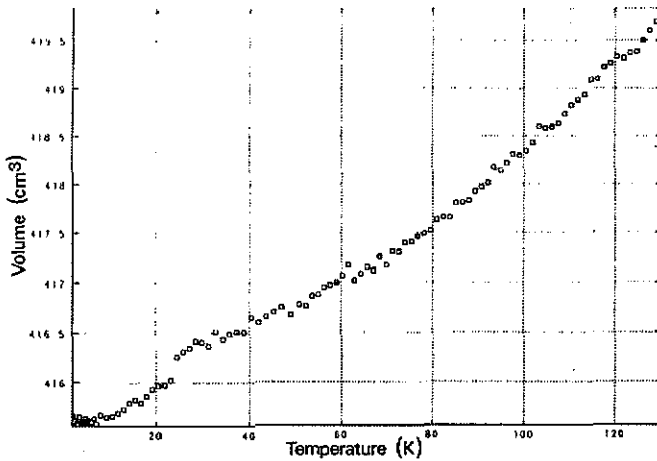


Figure 6. Evolution of the unit cell volume of HoMn_2 between 1.5 K and 128 K. The small anomaly seen at 25 K may be related either to the spin reorientation or to the Curie temperature.

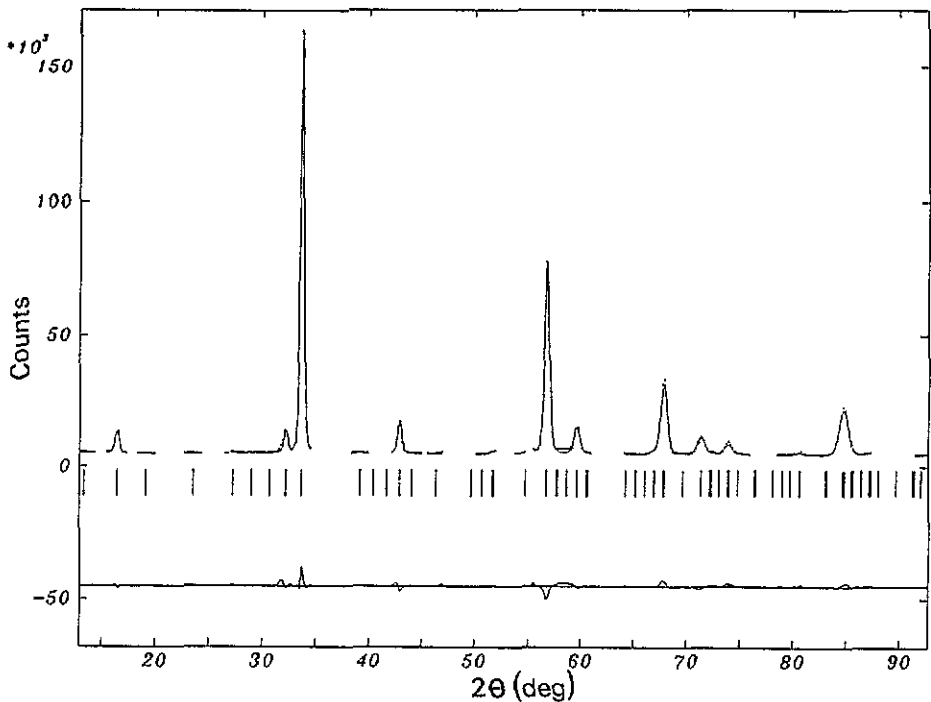


Figure 7. Observed, calculated and difference powder neutron diffraction profiles of HoMn_2 at 1.5 K assuming a magnetic moment on every fourth Mn site.

gives the final values for the magnetic moments, the lattice constants and the R factors. The values of this fit have to be compared to those of DyMn_2 [4], where the rare-earth moment of $\mu_{\text{Dy}} = 8.8 \mu_{\text{B}}$ was composed of a ferromagnetic part of $6.5 \mu_{\text{B}}$ and an antiferromagnetic one of $6.0 \mu_{\text{B}}$. One remarks that the ferromagnetic

component in HoMn₂ is increased slightly to 7.0 μ_B, while the antiferromagnetic one has decreased strongly to 3.5 μ_B. As it is this antiferromagnetic order which induces a magnetic moment on one fourth of the Mn sites it is not surprising to see the value found in HoMn₂ with μ_{Mn} = 0.6 μ_B significantly smaller than the corresponding one in DyMn₂, where μ_{Mn} = 1.4 μ_B.

4. Conclusion

The crystal structure of HoMn₂ remains cubic *Fd3̄m* below the magnetic transition temperature. The rare-earth sublattice assumes a spin-canted ferromagnetic order below the Néel point (31 K) and the Curie point (28 K). Consequently, the chemically equivalent Mn sites of the compound become magnetically inequivalent with one fourth having an induced moment of 0.6 μ_B. This is consistent with previous results on DyMn₂ [4] and with the idea of a critical distance, $d_c = 2.66 \text{ \AA}$, for the Mn–Mn near-neighbour separation, $d_{\text{Mn–Mn}}$, below which any Mn moment can only be of induced character. Contrary to compounds like TbMn₂, YMn₂, PrMn₂ with $d_{\text{Mn–Mn}} > d_c$, DyMn₂ ($d_{\text{Mn–Mn}} = 2.66 \text{ \AA}$), and now HoMn₂ ($d_{\text{Mn–Mn}} = 2.64 \text{ \AA}$), see the Mn moment induced by the antiferromagnetic component of the rare-earth sublattice magnetization. The magnitude of the induced moment seems to depend on the strength of this AF coupling and therefore decreases as we go from DyMn₂ to HoMn₂. It is not clear why the results we present here, while in agreement with those of Chamberlain [7], should differ so markedly from the diffraction patterns presented by Hardman *et al* [6]. We noted in section 3.1 that there was clear evidence of internal strain ($\epsilon = 2 \times 10^{-3}$) in the high-resolution patterns of HoMn₂. It is possible that internal strain may play an important role in defining the details of the magnetic structure of HoMn₂ in particular, and of the *RMn*₂ compounds in general, thereby introducing a new parameter into models of Mn local-moment formation and long-range magnetic order in these materials. However, as we have no estimate of the internal strain in the HoMn₂ sample of Hardman *et al*, we cannot assess whether the magnetic structure we derive here, or that reported in [6], better represents the 'true' magnetic ground state of HoMn₂. We intend to explore this problem further.

References

- [1] Shiga M 1988 *Physica B* 149 293
- [2] Shiga M, Wada H and Nakamura Y 1983 *J. Magn. Magn. Mater.* 31–34 119
- [3] Yoshimura K, Shiga M and Nakamura Y 1986 *J. Phys. Soc. Japan* 55 3585
- [4] Ritter C, Kilcoyne S H and Cywinski R 1991 *J. Phys.: Condens. Matter* 3 727
- [5] Shimizu K, Dhar S K, Vijayaraghavan R and Malik S K 1981 *J. Phys. Soc. Japan* 50 1200
- [6] Hardman K, Rhyne J J, Malik S K and Wallace W 1982 *J. Appl. Phys.* 53 1944
- [7] Chamberlain J R 1977 *Physica B* 86–88 138
- [8] Ritter C, Mondal S, Kilcoyne S H, Cywinski R and Rainford B D 1992 *J. Magn. Magn. Mater. (Proc. ICM '91)* at press
- [9] Ritter C, Mondal S, Kilcoyne S H and Cywinski R 1992 in preparation
- [10] Mondal S, Cywinski R, Kilcoyne S H, Rainford B D and Ritter C 1992 *J. Magn. Magn. Mater. (Proc. ICM '91)* at press
- [11] Mondal S, Cywinski R, Kilcoyne S H, Rainford B D and Ritter C 1992 *Physica B (Proc. ICNS '91)* at press
- [12] Mondal S, Cywinski R, Kilcoyne S H, Rainford B D and Ritter C 1992 *Physica B (Proc. ICNS '91)* at press
- [13] David W J F, Akporiaye D E, Ibberson R M and Wilson C C RAL 1988 *Internal Report RAL-88-103*
- [14] Rodriguez J, Anne M and Pannetier J 1987 *Institut Laue-Langevin Report* 87RO14T